VERSITA

OPTO-ELECTRONICS REVIEW **19**(2), 0–0

DOI: 10.2478/s11772-011-0003-9

Beam properties of fully optimized, table-top, coherent source at 30 nm

K. JAKUBCZAK*[1,2], T. MOCEK[1], B. RUS[1], J. POLAN[1], J. HREBICEK[1], M. SAWICKA[1], P. SIKOCINSKI[1], J. SOBOTA[3], T. FORT[3], and L. PINA[2]

[1]Department of Diode-pumped Lasers, Institute of Physics AS CR, 2 Na Slovance Str., 182 21 Prague, Czech Republic
[2]Faculty of Nuclear Sciences and Physical Engineering, Czech Technical University in Prague, 2 V Holesovickach Str., 182 21 Prague, Czech Republic
[3]Institute of Scientific Instruments AS CR, 147 Kralovopolska Str., 612 64 Brno, Czech Republic

We present results on development and experimental implementation of a 1-kHz, coherent extreme ultraviolet (XUV) radiation source based on high-order harmonic generation of the femtosecond, near-infrared laser pulses produced by the titanium-doped sapphire laser system (35 fs, 1.2 mJ, 810 nm) at the Institute of Physics AS CR / PALS Centre. The source comprises a low-density static gas cell filled with a conversion medium, typically argon. The comprehensive optimization of the XUV harmonic source has been performed with respect to major parameters such as gas pressure in the cell, cell length, position of the focus of the driving laser field with respect to the gas cell position, size of the driving near-infrared laser beam, chirp of the femtosecond pulse, and the focal length of the lens deployed in the experimental setup. Harmonic spectra were recorded using an XUV transmission grating spectrometer developed specifically for this purpose. Detailed characterization of the XUV source has been performed including measurement of the XUV beam profile, M^2 parameter of the beam, absolute energy, and spatial coherence.

Keywords: laser applications, high-order harmonic generation, coherent extreme ultraviolet radiation, ultrafast optics.

1. Introduction

The existing Ne-like zinc X-ray laser (XRL) at the Institute of Physics (IoP) of the Academy of Sciences of the Czech Republic (AS CR) and Prague Asterix Laser System (PALS) Research Centre emits coherent radiation at 21 nm and it is capable of delivering energy of up to a few-mJ in a single shot [1]. Despite recent progress in scientific applications of the energetic XRL [2], its practical use is severely limited by the driving iodine laser system which has repetition rate of 1 shot per 30 minutes. Therefore it is desirable to complement the existing XRL by a highly repetitive source of coherent XUV radiation based, e.g., on high-order harmonic generation (HHG) of the driving laser field. In case of HHG, the rather low single-shot energy (~nJ) is compensated by the repetitive operation of the source (typically up to ~kHz, Ref. 3). It is also possible to easily adjust spectral characteristics of the source to obtain a narrow spectral line at desired XUV wavelength. Additionally, since high-order harmonics inherit their properties from the driving laser field they are linearly polarized, feature Gaussian beam profile, and they are fully coherent. Moreover, ultrashort pulse duration of the emitted radiation is an important advantage for time-resolved investigation of physical processes which natural time scale is of the order of femtoseconds (1 fs = 10^{-15} s) or even less. Details on the physics underlying HHG process can be found elsewhere [4]. In this paper we focus on experimental implementation, characterization, and optimization of compact HHG source at 30 nm.

2. Experimental setup

The XUV source based on HHG was implemented at IoP/PALS. The experimental setup involves commercially available chirped pulse amplification (CPA) – based Ti-doped sapphire laser system (Coherent Inc.) delivering near-infrared (NIR) pulses with the following parameters E = 1.2 mJ, Δt = 35 fs, λ_c = 810 nm, repetition rate 1 kHz, and beam diameter (FWHM) 10 mm. The schematic drawing of the experimental setup is presented in Fig. 1. Initially, the NIR beam size is defined by an iris. Subsequently, it is focused by a dispersion corrected lens from fused silica or MgF_2. Lenses with a focal length of 750 mm, 1000 mm, and 1500 mm were used in the experiment. A gas cell was placed in the vicinity of the focal spot. The resulting HHG beam, being collinear with the driving NIR beam, was spatially clipped by an iris and filtered out using high quality aluminium foil of a proper thickness to adjust the XUV signal level to match the detector dynamic range.

*e-mail: kkjakubczak@gmail.com

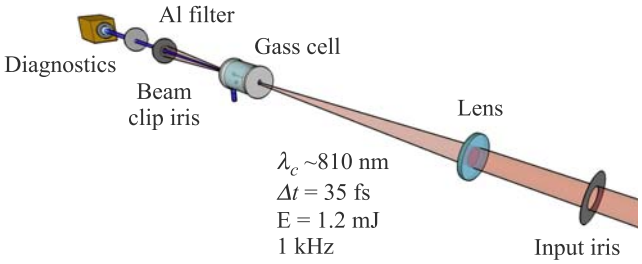

Fig. 1. Experimental setup of HHG source with a gas cell.

The design of the cell allows changing its length. It is mounted on XYZ motorized stage for easy manipulation under vacuum during the experiment. The inner part of the cell is made of a transparent material for easy viewing. The gas cell is connected to the pressure controller (P-602CV-AGD-33-V-350A Bronkhorst High-Tech BV) which supplies the cell with the gas at desired constant pressure. For HHG source optimization, argon gas as a conversion medium was used.

The main diagnostics for the characterization of the HHG source were high-resolution XUV detector for M^2 parameter measurement and transmission grating spectrometer (TGS) for characterization in the spectral domain. The XUV detector (Pixelink PL-A781) is based on CMOS technology chip featuring size of 2/3" and resolution of 3000× 2200 pixels (3.6×3.6 μm pixel size). The chip covering glass has been removed and the sensor has been covered with 5 μm-layer of P43 phosphor. The camera is enclosed in stainless steel housing for vacuum compatible operation.

For high-precision spectral measurements, TGS was used. The spectrometer comprises a flat relay mirror and an imaging spherical mirror (both Au-coated, diameter 2", deployed in grazing incidence geometry). The dispersion element is a free-standing transmission grating (2500 lines/mm, silicon nitride; nm^2 LLC). XUV spectrum was detected with an X-ray charge coupled device (CCD) camera (Andor DX440-DN). Special software was coded for TGS calibration, design of the experimental setup, and evaluation of spectral characteristics of the spectrometer.

During the experiments, TGS was set up to measure a spectrum in the range below ~60 nm with resolution < 1 Å. The distance between spherical mirror and the source was ~1 m, distance between spherical mirror and grating was 140 mm, distance between grating and detector was 300 mm, the source size was assumed to be 100 μm, and transmission grating period was 400 nm with a line width of 205 nm, the radius of spherical mirror R = 1700 mm, the grazing incidence angle onto spherical mirror $\varphi = 12°$. The theoretical estimation of TGS spectral resolution was confirmed by experimental results.

The absolutely calibrated X-ray CCD camera by Andor has been used for the estimation of the total HHG signal (preceded only with beam clip and an Al filter) and for the XUV beam profile measurements. The camera has a 2048× 512 pixels matrix. The pixel size is 13.5×13.5 μm resulting in matrix dimensions of 27.6×6.9 mm.

3. Experimental results

The harmonic source was first optimized and the influence of optimization parameters on the source properties was investigated. Secondly, further characterization of the beam properties was performed.

The denotations used throughout this paper are, L is the gas cell length, p is the pressure inside the gas cell, f is the focal length of the lens, d is the diameter of the entrance iris (in front of the lens), df/dt is the position of the motor of one of the gratings inside the compressor which movement changes the chirp of the pulse, H25 stands for the 25th harmonic order, H27 for the 27th, etc.

In order to minimize measurement errors due to shot-to-shot fluctuation, integration time was set typically to 0.5 s (at 1 kHz repetition rate of the laser). Moreover, for each measurement point always three separate images were taken (e.g. spectrum). The background was subtracted and the three images were averaged. To obtain spectrum, lineout selection rectangle was defined with dimensions 50×2048 px. The rectangle was vertically centred at the maximum intensity of the spectral lines. Within the rectangle, the data was averaged along columns of the rectangle resulting in a set of 2049 items. The measurement error never exceeded 10%.

3.1. Optimization of source parameters

The first experimental campaign was related to comprehensive characterization of the HHG source and its optimization. The parameters under investigation were chirp of NIR femtosecond laser pulse, NIR beam size, focal length of the lens, gas cell length, gas pressure, and cell position.

3.1.1. Chirp of NIR femtosecond laser pulse

Optimization of the source chirp has been performed in the setup presented in Fig. 1. TGS was used as a main diagnostic tool. Selected experimental results are presented in Fig. 2. The two strongest spectral lines were the 27th and the 25th harmonics. The source was optimized with the parameters f = 750 mm, L = 12 mm, d = 11 mm, and p = 40 mbar. All graphs are normalized to 0.5-s integration time and 0.8-μm thickness of Al filter.

Spectral characteristics from optimization of the 27th harmonic order *vs*. chirp of the driving field are presented in Fig. 2(a). Since kinetic energy of the tunnel-ionized electron in HHG process depends on the phase of the driving field, apart from changes in intensity, well known spectral shift of the spectral peak is observed [4]. Wavelength-calibrated changes of the intensity during the chirp scan are presented in Fig. 2(b). During the scan, the shift in wavelength by 0.23 nm from optimal conditions (at 30.1 nm) caused a signal drop by 83%.

3.1.2. Size of NIR driving beam

The geometrical component to the phase mismatch vector, having its origin in the Gouy phase shift in the region of the focus, can be minimized by changing the confocal parame-

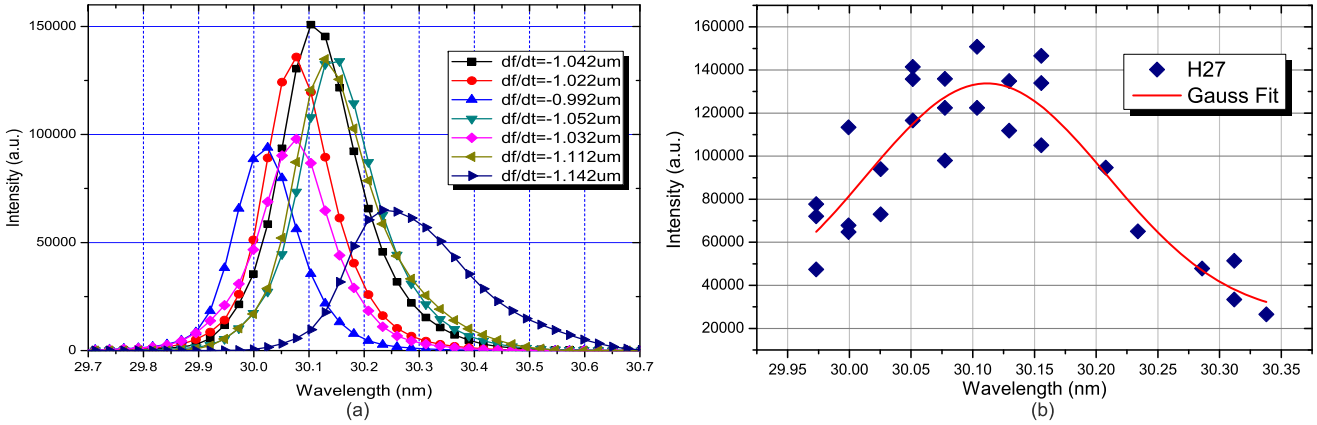

Fig. 2. Optimization of driving NIR field chirp during HHG: (a) peak of the 27th harmonic order spectrally shifts while chirp is tuned. Instead of real instantaneous frequency, units in relative positions of the compressor grating are given as a parameter and (b) intensity drop during spectral line tuning is observed.

ter. Since a focal spot size is a function of the beam diameter, experimentally, the changes of the confocal parameter are obtained by changing the driving field beam size through adjusting the opening of the aperture placed at the beginning of the beamline.

The experimental results are presented in Fig. 3. Optimal size of the aperture was found to be 11 mm. Experimental conditions were f = 750 mm, L = 12 mm, and p = 45 mbar. To keep the intensity constant in the interaction region while increasing a focal length of the lens in HHG setup, increase in laser intensity is required. This was found to be an issue in the described experimental setup (due to limited output parameters of the available laser system).

Typical dependence of the harmonic signal *vs*. the aperture size was observed [4]. For small iris opening (in this case below 9 mm), the signal is very low. Then, the signal suddenly raises and reaches its maximum (at 11 mm iris opening). Finally, a drop of the spectral intensity is observed. Out of the optimum, for higher beam sizes, the spectral intensity is preserved at moderate level and does not change any further.

3.1.3. Focal length of a lens

Intensity of the driving NIR beam in the interaction region is a very important factor since in HHG from gases it is desired to adjust intensity level, so as to create favourable conditions for tunnelling the most outer electrons of the atomic gas. If the intensity is too low, very low number of electrons will be tunnel-ionized providing low contribution to generated XUV signal. On the other hand, if the intensity is too high, very high density of free electrons will be created. These electrons will defocus NIR beam and become a source of de-phasing of NIR and depletion of the intensity of the NIR pulses. Additionally, in the gas cell arrangement, for efficient HHG self-channelling is desired. It is achieved by the proper combination of laser intensity and gas pressure leading to interplay between intensity-induced self-focusing and free-electron-induced defocusing of the driving laser beam.

The experimental results on scan of the focal length of the lens involved for 27th harmonic order at 30 nm are presented in Fig. 4. Experimental conditions were A: d = 11 mm, p = 40 mbar, B: d = 13 mm, p = 25 mbar, C: no H27 signal was recorded for any parameters combination. The

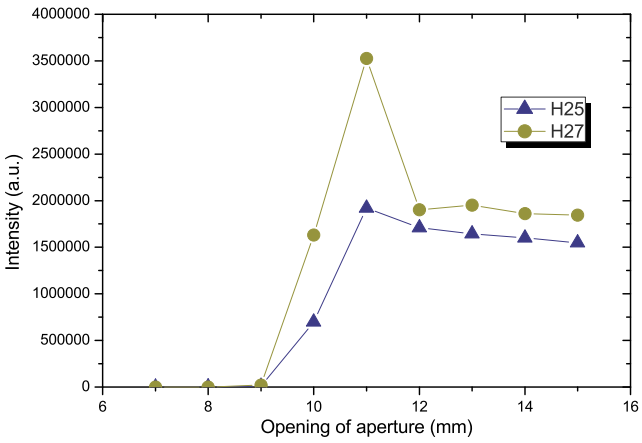

Fig. 3. Optimization of a driving beam size.

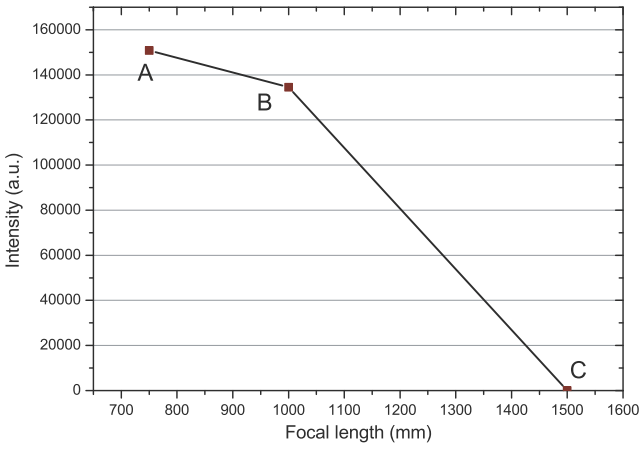

Fig. 4. Optimization of a focal length of a lens for H27.

cell length was 12 mm. The strongest signal yield was recorded for f = 750 mm, which is, however, just 15% higher than that for f = 1000 mm. Even stronger harmonic yield might be expected for f < 750 mm but this measurement was not feasible due to vacuum system limits.

3.1.4. Gas cell length

In order to maximize the interaction length between the NIR beam and conversion medium up to the values where signal decays due to re-absorption of the XUV radiation by neutral gas, optimization of gas cell length was performed. Experimental results are displayed in Fig. 5. The optimal gas cell length for f = 1000 mm was found to be 10 mm.

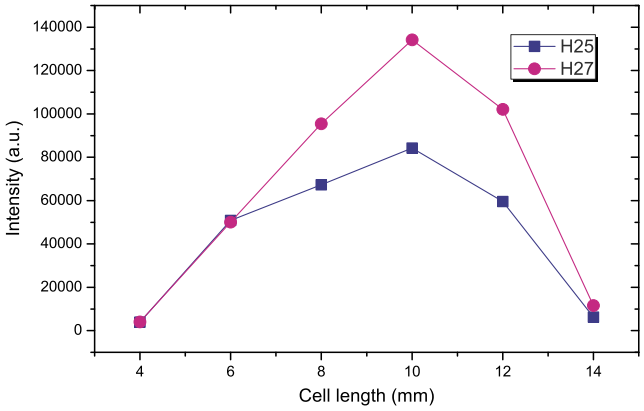

Fig. 5. Optimization of a gas cell length for f = 1000 mm.

3.1.5. Gas pressure

It has been experimentally confirmed that intensity of the m^{th} harmonic order is proportional to the square of the atomic density ($I_m \propto N^2$) accounting for the coherent character of HHG process [5]. On the other hand, it has to be noted that $I_m \propto |F_m|^2$, where F_m is so-called phase matching factor rapidly decreasing with m [4]. This is the reason of rapid decrease in spectral intensities in the long-wavelength part of the harmonic spectrum. Thus, a proper choice of the gas pressure is crucial for the efficient HHG process.

Selected experimental results are presented in Fig. 6. Dependence between signal yield and the gas pressure presents typical optimal conditions for the value of the pressure. Optimal pressure for the lens f = 750 mm was ~45 mbar and for f = 1000 about 25 mbar.

3.1.6. Cell position

The optimization of the position of the gas cell along the driving NIR beam caustic was performed in order to minimize the geometrical component of the phase mismatch vector. The "0" position of the motorized stage corresponds to the beam waist location close to the entrance to the cell. The experimental results are presented in Fig. 7.

It could be observed that in general two maxima exist: when the beam waist is close to both ends of the cell. However, more favourable conditions are with the focus located at the end face of the cell (along beam propagation direction) [6].

3.2. HHG beam profile

The experimental conditions for the measurement of the XUV beam profile of the optimized harmonic source were: diameter of the aperture limiting the NIR laser beam d = 11 mm, focal length of the lens f = 750 mm, gas cell length L = 12 mm, gas pressure p = 45 mbar, Δt = 35 fs, λ_c = 810 nm, 1.2 mJ at 91 Hz. Integration time was 3 s. The measurement was performed using Andor X-ray CCD camera. The distance between CCD and the front face of the gas cell was 2157 mm. A 400-nm Al filter (Luxel) was placed in front of the camera.

The measured HHG beam footprint is shown in Fig. 8. Gaussian fit was done with a fit coefficient higher than 99% in both directions (Fig. 9). The beam size at the distance given by camera position was 2.86 mm and 2.49 mm (FWHM) in horizontal and vertical directions, respectively.

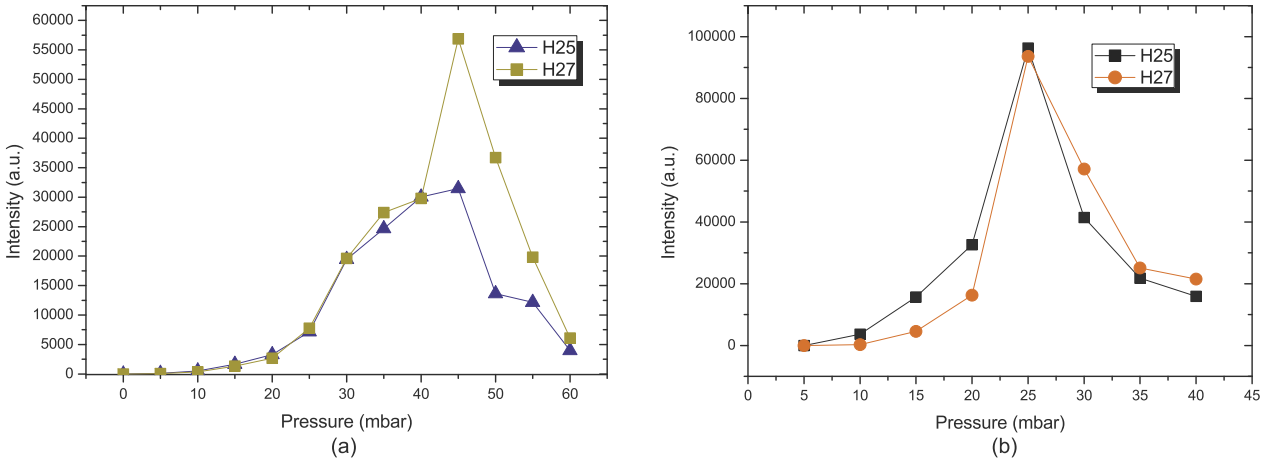

Fig. 6. Optimization of gas pressure (Ar). Focal length of a lens was: (a) f = 750 mm and (b) f = 1000 mm. The length of a gas cell L = 12 mm in both cases, while in (a) d = 10 mm and in (b) d = 13 mm.

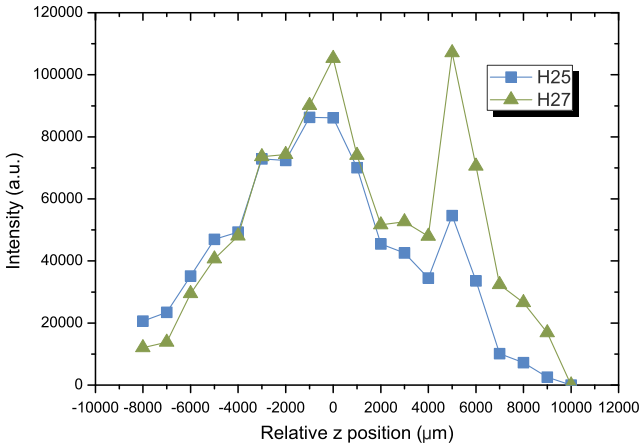

Fig. 7. Optimization of longitudinal gas cell position. Experimental conditions are shown in the figure.

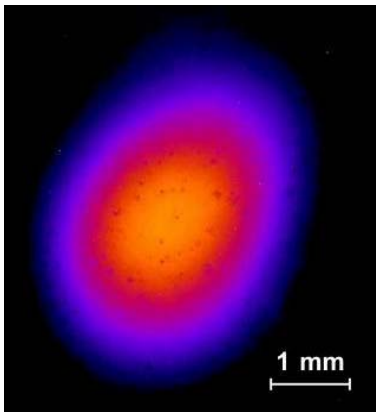

Fig. 8. High-order harmonic beam profile recorded by X-ray CCD camera at 2157 mm away from a source.

The HHG beam exhibits very smooth and homogeneous intensity distribution, and does not feature any significant asymmetry or non-uniformities like most of current X-ray lasers (c.f. Ne-like Zn soft X-ray laser, Ref. 1 or capillary discharge soft X-ray laser, Ref. 7).

3.3. M^2 of XUV beam

The measurement of the quality factor (M^2) of the HHG beam was performed in a standard scheme when the beam is focused, however, in the XUV spectral region as shown in Fig. 10. The NIR beam was first filtered out by 400 nm Al filter (Luxel), and then, the XUV beam was focused by a prototype spherical multilayer (ML) C/Si mirror (R = 30% at 30 nm, $\beta = 6°$, f = 250 mm, the number of layers N = 20, the multilayer period d = 16.6 nm) which has been designed at IoP and manufactured at the Institute of Scientific Instruments in Brno, Czech Republic. The distance between the exit of gas cell and ML mirror was about 2295 mm. The caustic was directly measured with an XUV CMOS Pixelink camera. The initial "0" position of the camera was at the distance of ~280 mm from the ML mirror along beam propagation path. The experimental conditions for the HHG source were p = 45 mbar, the NIR beam diameter d = 11 mm, the gas cell length L = 12 mm, the focal length of the lens f = 750 mm, λ_c = 810 nm, Δt = 35 fs, E = 1.2 mJ at a repetition rate of 1 kHz. Signal acquisition time was 50 ms.

By scanning the HHG beam profile it was possible to measure the XUV beam radius and to obtain the beam caustic (Fig. 11). The estimated values of a beam quality factor at central wavelength of 30 nm were: $M_x^2 = 4.64$ (H - horizontal direction) and $M_y^2 = 38.45$ (V – vertical direction). Values of M^2 factor greater than 3 are typical for multimode beams, thus, recalling the results of the measurements of the beam profile it is assessed that estimated values of M_x^2 and M_y^2 do not reflect the beam quality but rather low grade of the focusing optics which distorts the beam. Moreover, longitudinal asymmetries of the beam caustic and very strong astigmatism were observed.

For estimation of the maximum achievable XUV intensity, the focus of the smallest area, which amounts to 3.4×10^{-5} cm^2, was taken. For the harmonic beam energy of ~0.7 nJ (as discussed later in this paper) and average reflectivity of the ML mirror of 25% at 30 nm [8], the resulting

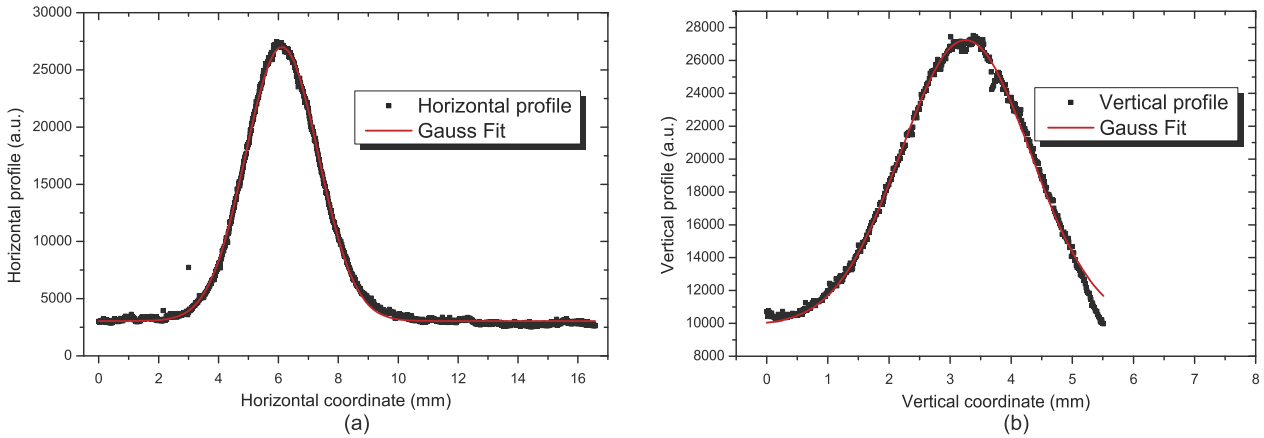

Fig. 9. XUV beam profile lineouts in: (a) horizontal and (b) vertical directions. Black points present measurement data while red curves are their Gaussian fits. In both cases, a fit coefficient exceeded 99%.

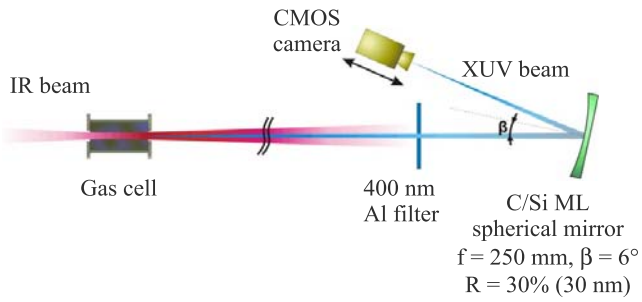

Fig. 10. Experimental setup for measurement of M^2 parameter of HHG beam.

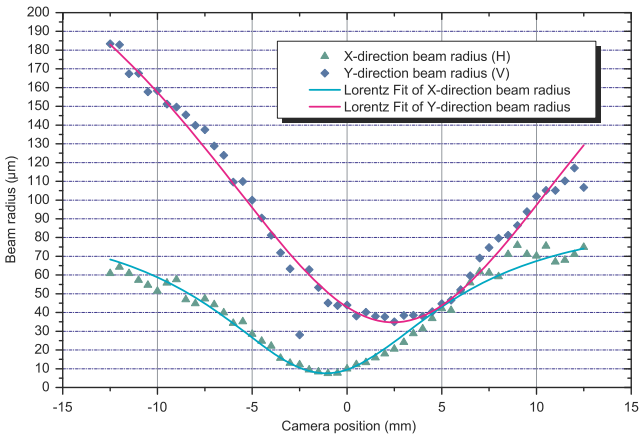

Fig. 11. Caustic of focused XUV beam. Positive values mean moving a detector away from focusing ML mirror.

XUV (all harmonic orders) fluence in the focus is about 5×10^{-6} J/cm^2. If we assume, the XUV pulse duration of 35 fs, the intensity in the focus would be 1.4×10^8 W/cm^2. Improvement in terms of intensity in the focus could be obtained by moving the camera into circle of least confusion where, according to simulations presented in Ref. 6, the intensity can increase by a factor of 2.4. Alternatively, aspherical or off-axis paraboloidal mirror can be used.

3.4. HHG beam spatial coherence

The estimation of the XUV beam spatial coherence for optimized HHG source was performed in a double-slit Young's experiment. The experimental setup is shown in Fig. 12. NIR laser beam (λ_c = 810 nm, Δt = 35 fs, E =1.2 mJ, 1 kHz and beam limiting aperture size of 11 mm) was focused by a lens (f = 750 mm, not visible in the figure) into a gas cell (Ar, p = 45 mbar, L = 12 mm) resulting with HHG. The longitudinal position of the cell was optimized to maximize XUV total signal (focus positioned in the vicinity of the cell exit). A 400-nm Al filter (Luxel) followed by a Ni foil with a set of pairs of slits (Optimask S.A.). The pairs were 20 μm wide and 1 mm high. The separation between the slits ranged from 0 (one slit) to 500 μm with a step of 50 μm allowing precise scan across the XUV beam. The interference fringes were recorded with Andor X-ray CCD camera.

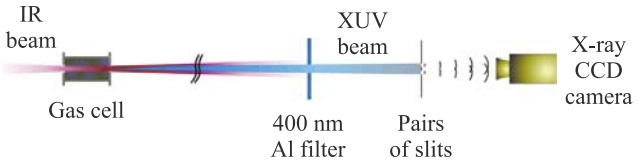

Fig. 12. Experimental setup for measurement of spatial coherence of high-order harmonic beam.

The distance between front face of the cell and the slits was 1560 mm, while the distance between slits and CCD camera was 597 mm. The position of the HHG beam was centred between a pair of slits actually used in the experiment.

Examples of the interference fringes recorded in the measurement are shown in Fig. 13.

Fringes visibility as a function of a distance between the slits was evaluated and plotted in Fig. 14. The visibility of the fringes is the highest (above 90%) for inner part of the beam of a diameter ~120 μm, while 50% drop of visibility was observed for a diameter of ~200 μm. Since the maximum slits separation is smaller than the total beam diameter (2.86×2.49 mm, FWHM) it is only possible to claim that according to commonly used criterion of $1/e^2$, the harmonic beam is fully coherent for a diameter not smaller than 500 μm (for 500 μm distant slits μ = 29.4%). It was not possible to match the beam size and the maximum slits separation in the setup due to limits of the vacuum system.

3.5. Estimation of absolute HHG energy

The estimation of the absolute energy carried by the HHG beam was performed for the following experimental conditions: E = 1.2 mJ, λ_c = 810 nm, Δt = 35 fs, repetition rate of 91 Hz, acquisition time 3 s, iris size 11 mm, Ar pressure 45 mbar, the cell length L = 12 mm, optimized longitudinal position (focus in the vicinity of the back face of the cell), and the focal length of the lens f = 750 mm. Andor X-ray CCD camera was used to record the data.

The total energy per single pulse carried in all harmonic orders is estimated to be 0.7 nJ and 0.09 nJ in a single spectral line at 30 nm (the strongest harmonic order in the spectrum) resulting in conversion efficiency of 5.4×10^{-7} and 7.1×10^{-8}, respectively. Since standard operation regime of the source involves a repetition rate of 1 kHz of the driving laser, the accumulated signal in all harmonics is 0.652 μJ/s.

4. Conclusions

The results, presented in this paper, extensively characterize table-top source of coherent XUV radiation based on the interaction of femtosecond laser pulses with an argon-filled gas cell via high-order harmonic generation process. A comprehensive optimization of major HHG beam parameters has been performed. The ultrafast, coherent XUV beamline developed at IoP/PALS now routinely operates at 1 kHz and presents a complementary device to the existing highly energetic XRL at 21.6 nm. It already serves for first

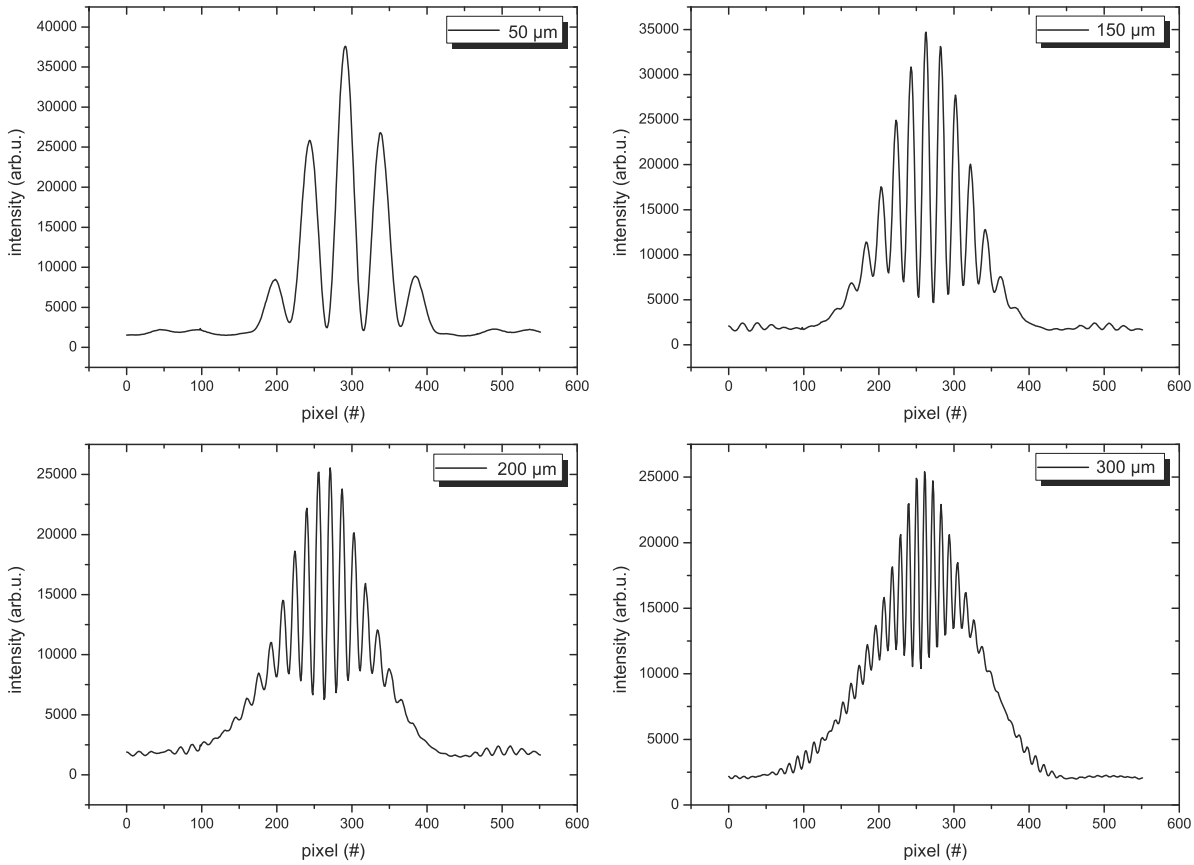

Fig. 13. Recorded interference patterns from 50, 150, 200, and 300 µm distant slits (separation shown in the graphs).

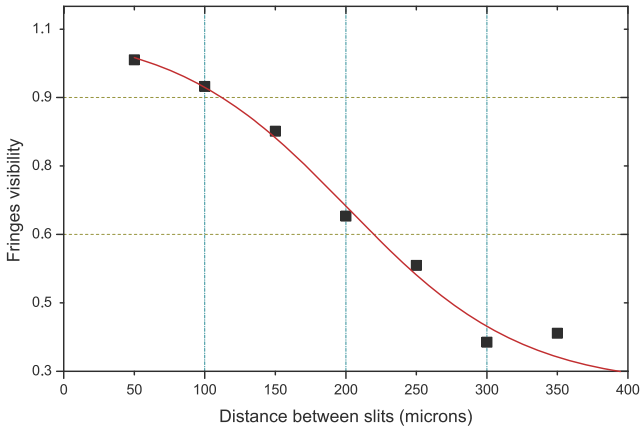

Fig. 14. Interference fringes visibility as a function of a distance between a pair of slits.

practical applications such as XUV multilayer optics metrology and processing of materials.

Acknowledgements

This research was supported by the Czech Science Foundation (Grant 202/07/J008), the Czech Ministry of Education (Grant LC528), and the Academy of Sciences of the Czech Republic (Grants M100100911, KAN300100702 and Z10100523).

References

1. B. Rus, T. Mocek, A.R. Präg, M. Kozlová, G. Jamelot, A. Carillon, D. Ros, D. Joyeux, and D. Phalippou, "Multi-millijoule, highly coherent x-ray laser at 21 nm operating in deep saturation through double-pass amplification", *Phys. Rev.* **A66**, art. No. 063806 (2002).
2. T. Mocek, B. Rus, M. Kozlova, J. Polan, P. Homer, K. Jakubczak, M. Stupka, D. Snopek, J. Nejdl, M.H. Edwards, D.S. Whittaker, G.J. Tallents, P. Mistry, G.J. Pert, N. Booth, Z. Zhai, M. Fajardo, P. Zeitoun, J. Chalupsky, V. Hajkova, and L. Juha, "Plasma-based X-ray laser at 21 nm for multidisciplinary applications", *Eur. Phys. J.* **D54**, 439–444 (2009).
3. M. Schultze, E. Goulielmakis, M. Uiberacker, M. Hofstetter, J. Kim, and D. Kim, "Powerful 170-attosecond XUV pulses generated with few-cycle laser pulses", *New J. Phys.* **9**, 243 (2007).
4. P. Jaeglé, *Coherent Sources of XUV Radiation. Soft X-Ray Lasers and High-Order Harmonic Generation*, Springer, 2006.
5. X.F. Li, A. L'Huillier, M. Ferray, L.A. Lompré, and G. Mainfray, "Multiple-harmonic generation in rare gases at high laser intensity", *Phys. Rev.* **A39**, 5751–5761 (1989).
6. K. Jakubczak, "Development and applications of coherent XUV sources driven by ultrashort laser pulses", *PhD Dissertation*, Czech Technical University, Prague, 2010.
7. J.J. Rocca, "Table-top soft x-ray lasers", *Rev. Sci. Instrum.* **70**, 3799 (1999).
8. Centre for X-ray optics, http://www.cxro.lbl.gov/

